

UC Irvine

UC Irvine Previously Published Works

Title

Neutron scattering study of the magnetic transition in $(\text{Ho}_{1-x}\text{Er}_x)\text{Rh}_4\text{B}_4$ alloys

Permalink

<https://escholarship.org/uc/item/7h2398dz>

Journal

Physical Review B, 25(1)

ISSN

0163-1829

Authors

Mook, HA
Koehler, WC
Maple, MB
et al.

Publication Date

1982

DOI

10.1103/PhysRevB.25.372

Copyright Information

This work is made available under the terms of a Creative Commons Attribution License, available at <https://creativecommons.org/licenses/by/4.0/>

Peer reviewed

Neutron scattering study of the magnetic transition in $(\text{Ho}_{1-x}\text{Er}_x)\text{Rh}_4\text{B}_4$ alloys

H. A. Mook and W. C. Koehler

Solid State Division, Oak Ridge National Laboratory, Oak Ridge, Tennessee 37830

M. B. Maple, Z. Fisk, D. C. Johnston,* and L. D. Woolf*

Institute for Pure and Applied Physical Sciences, University of California, San Diego, La Jolla, California 92093

(Received 10 August 1981)

Using neutron scattering techniques we have examined the magnetic transitions for compounds in the $(\text{Ho}_{1-x}\text{Er}_x)\text{Rh}_4\text{B}_4$ pseudoternary system. We find a wide variety of behavior ranging from mean-field behavior for HoRh_4B_4 to complicated behavior with more than one type of ordering for $\text{Ho}_{0.3}\text{Er}_{0.7}\text{Rh}_4\text{B}_4$. Our results for the pseudoternary compounds are consistent with a model in which Ho orders along the c axis with nearly its free-ion moment, while Er orders in the basal plane, but with a moment reduced from the free-ion value. Ordering along the c axis results in the destruction of superconductivity in a sharp transition at the same temperature that a sharp spike appears in the heat capacity. Because Ho and Er have competing orthogonal magnetic anisotropies, pseudoternary compounds near the composition $\text{Ho}_{0.3}\text{Er}_{0.7}\text{Rh}_4\text{B}_4$ are near a multicritical point in the magnetic phase diagram.

INTRODUCTION

Since the discovery of reentrant superconductivity in ErRh_4B_4 (Ref. 1) and $\text{Ho}_{1.2}\text{Mo}_6\text{S}_8$ (Ref. 2) there has been considerable interest in the nature of the magnetic transitions in these types of materials. This interest has been reemphasized recently with theoretical predictions for a number of different kinds of magnetic states in the neighborhood of the magnetic transition.³⁻¹⁴ The $(\text{Ho}_{1-x}\text{Er}_x)\text{Rh}_4\text{B}_4$ pseudoternary system is an ideal system in which to study the interaction between magnetism and superconductivity since a wide variety of phenomena occur throughout the alloy system.¹⁵⁻²⁰ The low-temperature phase boundaries of this alloy system have been mapped

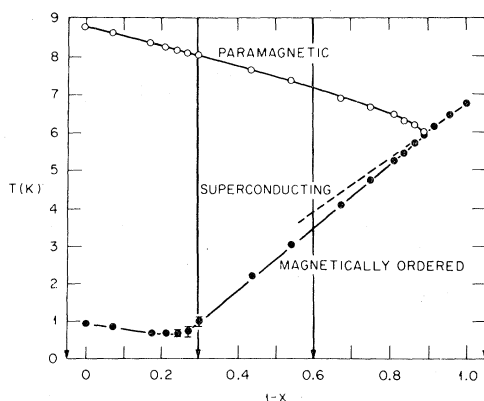


FIG. 1. Phase diagram for the $(\text{Ho}_{1-x}\text{Er}_x)\text{Rh}_4\text{B}_4$ pseudoternary system. The arrows show the compositions studied by neutron scattering.

out by Johnston *et al.*¹⁵ using ac magnetic susceptibility measurements, and a diagram of the phase boundaries is shown in Fig. 1. The compositions that we have investigated by neutron diffraction are shown by the arrows on the diagram. They represent the end points of the alloy system and the compositions $\text{Ho}_{0.6}\text{Er}_{0.4}\text{Rh}_4\text{B}_4$ and $\text{Ho}_{0.3}\text{Er}_{0.7}\text{Rh}_4\text{B}_4$.

The specific-heat anomalies at the transitions for these materials have been measured by MacKay *et al.*¹⁶ and have served as a guide for the materials we have chosen to measure. These specific-heat anomalies show a wide range of behavior and we will compare our neutron scattering results closely with the specific-heat results. We will see that the neutron results can be used to help interpret the specific-heat results, and the two sets of measurements taken together give us quite a lot of information about the nature of the magnetic transitions in these materials.

EXPERIMENTAL TECHNIQUE

Except for ErRh_4B_4 where a single crystal is available, all measurements have been made on powdered polycrystalline material. The materials were prepared by arc melting the rare-earth tetraborides with Rh followed by annealing. The rare-earth tetraborides were prepared as small crystals by precipitation from molten Al which appeared to remove traces of carbon which were found in the as-received boron. The ^{11}B isotope was used to decrease the absorption cross section for slow neutrons.

The neutron scattering measurements were made

at the High Flux Isotope Reactor at Oak Ridge using the standard triple-axis spectrometers. The analyzing crystal was not used in the experiments, and the detector was set in the straight-through position so that the spectrometer was similar to a standard powder spectrometer. The neutron wavelength used was generally 2.349 Å and pyrolytic graphite was used as a monochromator and as a filter to remove higher order wavelength contamination. Some high-resolution work was done with a Be monochromator and fine collimation to resolve closely spaced peaks and to measure the spatial extent of the observed magnetic order. Unless stated differently the measurements discussed below were made with a pyrolytic graphite monochromator and 40' collimation. Neutron counting times were made versus a monitor counter placed in the reactor beam to account for any small variations in reactor power.

The structure of the ternary borides was determined by Vandenberg and Matthias.²¹ They found that the space group was $P4_2/nmc$. There are two formula units of $R\text{Rh}_4\text{B}_4$ per unit cell where R is a rare-earth atom. The structure was assumed to have 8 Rh in the (8g); 0, x , z , etc. positions and 2 R in the (2b); 0, 0, $\frac{1}{2}$; $\frac{1}{2}$, $\frac{1}{2}$, 0 positions. The B atoms were also placed in the eightfold 8g positions. They found the best fit was obtained with $x_{\text{Rh}}=0.248$, $z_{\text{Rh}}=0.137$ and $x_{\text{B}}=0.325$, and $z_{\text{B}}=0.847$. These parameters were further refined by Moncton *et al.*²² for ErRh_4B_4 to $x_{\text{Rh}}=0.253$, $z_{\text{Rh}}=0.148$ and $x_{\text{B}}=0.322$, $z_{\text{B}}=0.856$. These latter parameters are only slightly different than those obtained by Vandenberg and Matthias but were used to analyze our data for the $(\text{Ho}_{1-x}\text{Er}_x) \times \text{Rh}_4\text{B}_4$ alloy series. Satisfactory agreement was obtained in all cases by using the above parameters and an additional refinement was not found to be necessary.

The $P4_2/nmc$ space group then gives the following contributions to the nuclear structure factors for the various reflections. The R only contributes to the reflection of $h+k+l=2n$ in which case it contributes a structure factor of $2(-1)^l$ to the reflection. If $h+k+l$ is even, both the B and Rh have structure factor terms given by $4(\cos 2\pi hx + \cos 2\pi kx)\cos 2\pi lz$. If $h+k+l$ is odd the structure factor term is given by $-4i[(\cos 2\pi hx - \cos 2\pi kx)\sin 2\pi lz]$. These structure factor terms multiplied by the appropriate neutron scattering amplitudes and added together give the total structure factor for the reflection. The neutron scattering amplitudes used were $b_{\text{Rh}}=0.584$, $b_{\text{B}}=0.61$, $b_{\text{Ho}}=0.85$, and $b_{\text{Er}}=0.79$, all in the units of 10^{-12} cm. For the first reflection (101), we have for HoRh_4B_4 a R contribution of $-2(0.85)$, a Rh contribution of $(2.347)(0.584)$, and a B contribution of $1.391(0.61)$ for a total contribution of 0.5191. The nuclear intensity is then the square of the structure factor F^2 or 0.2695×10^{-24} cm².

The magnetic scattering is given by the square of

the magnetic structure factor F_m which can be written as²³

$$|F_m|^2 = 4 \left(\frac{\gamma e^2}{2mc^2} \right)^2 \mu^2 f(\vec{K})^2 [1 - (\hat{K} \cdot \hat{\mu})^2] \quad (1)$$

where

$$\left(\frac{\gamma e^2}{2mc^2} \right) = -0.2695 \times 10^{-12} \text{ cm} \quad .$$

μ is the magnetic moment, \vec{K} is the neutron momentum transferred to the crystal, $\hat{\mu}$ is the moment direction and $f(\vec{K})$ is the magnetic form factor.

If we assume the spin direction is along the c axis, $[1 - (\hat{K} \cdot \hat{\mu})^2]$ becomes equal to 0.66 for the (101) reflection. Actually this term is quite insensitive to whether the moment direction is parallel to the c axis or in the basal plane and thus the (101) reflection is not useful in determining the spin direction. The form factor $f(K)$ has not been measured for Ho in HoRh_4B_4 so that we have used the values of the Ho^{+3} and Er^{+3} form factors from Stassis *et al.*²⁴ The magnetic contribution to the (101) reflection for a c -axis ferromagnet is thus given by $0.172 \mu^2$. For a moment of $10\mu_B$ on the Ho we thus obtain a ratio of

$$\frac{F_m}{F_n} = \frac{17.2}{0.2695} = 63.8 \quad (2)$$

so that the magnetic scattering is much larger than the nuclear scattering for the (101) reflection. It turns out that the first three reflections (101), (110), (002) are mostly magnetic in nature. The first purely nuclear reflection is the (102) which is again small compared to the magnetic contribution to the (101) reflection. The magnetic reflections thus dominate the diffraction pattern when the material is in the ordered phase.

We have found ferromagnetism for all four compositions measured across the alloy phase for the lowest temperature magnetic state. All magnetic reflections thus coincide with the nuclear reflections and are based on the primitive cell. This makes the powder pattern analysis straightforward and the moment size and direction are easily found from the powder patterns. Small deviations from ferromagnetism could be overlooked in the patterns but these deviations would have to be on the order of a few percent or consist of very long-range oscillatory structures such that satellites would be hidden under the main diffraction peaks. No indications of this have been observed as all powder magnetic diffraction peaks for the lowest temperature are resolution limited. An oscillatory structure has been found for ErRh_4B_4 in the neighborhood of the magnetic transition and this will be discussed later in the paper.

Some impurity phases have been observed in the x-ray and neutron patterns of our sample materials. The extra diffraction lines can be attributed to RhB ,

RRh_3B_2 , RRh_6B_4 , and/or RB_4 phases. These impurity lines are small and do not affect the analysis of the data which is based on lines of the RRh_4B_4 cell. The observed impurity lines cannot be based on the RRh_4B_4 cell and thus it is assumed they have nothing to do with the structure of interest. We cannot rule out the possibility that a small noncollinear component of the magnetic structure is responsible for some of the lines, but we have seen no indication that this is the case. Straightforward analysis of the data show that a long-range ferromagnetic structure is consistent with the intensities observed for the RRh_4B_4 reflections at the lowest temperatures.

EXPERIMENTAL RESULTS

HoRh₄B₄

We can see from Fig. 1 that HoRh₄B₄ becomes magnetic at 6.74 K and does not become a superconductor at any temperature above 0.07 K. This compound has been previously studied using neutron diffraction measurements by Lander *et al.*²⁵ and the magnetic structure was found to be ferromagnetic with the magnetic moment aligned along the c axis. The extrapolated zero-temperature moment was found to be $8.7\mu_B$ which is nearly the full free-ion moment for Ho of $10\mu_B$. Our diffraction pattern for HoRh₄B₄ taken at 1.7 K is shown in Fig. 2. Large magnetic (101) and (110) diffraction peaks are visible but the (002) peak is missing. This means that $1 - (\hat{K} \cdot \hat{\mu})^2$ is equal to zero for this peak so that the magnetic moment alignment is along the c axis in agreement with the earlier measurement of Lander *et al.*²⁵ The diffraction pattern shows some small impurity lines but no indication of antiferromagnetic or spiral ordering is visible.

A careful measurement of the magnetic order parameter was not made in the earlier neutron diffraction work.²⁵ In fact the heat-capacity measurements^{16,26,27} indicate that the order parameter is quite interesting in this material. The heat capacity has a sawtooth-shaped feature arising from magnetic ordering that is nearly identical in both shape and magnitude to that expected for a mean-field ferromagnet. Equation (1) shows that the magnetic neutron scattering intensity of a reflection is proportional to the square of the ordered moment. Thus a measure of the intensity of the magnetic component of a reflection gives a direct measure of the ordered moment. Figure 3 shows the magnetic intensity of the (101) reflection plotted versus temperature. We see a smooth falloff of intensity that decreases directly to zero at the transition temperature of 6.80 K with no sign of rounding of the transition by critical fluctuations. The measured transition temperature of 6.80 K is in excellent agreement with the temperature of the sawtooth edge of the heat-capacity measurements.

Near the transition we can assume that the magnetic intensity I is given by

$$I \sim (T_c - T)^\alpha, \quad (4)$$

so that

$$\ln I \sim \alpha \ln(T_c - T). \quad (5)$$

Figure 4 shows a plot of $\ln I$ vs $\ln(T_c - T)$. The slope of the curve equals 1.08 ± 0.1 so that

$$I \sim (T_c - T)^{1.08 \pm 0.1}, \quad (6)$$

$$\mu \sim (T_c - T)^{0.54 \pm 0.05}. \quad (7)$$

The critical exponent expected from mean-field theory is 0.5 so that the neutron scattering results appear to be consistent with a mean-field nature of the transition. The range of validity of the mean-field

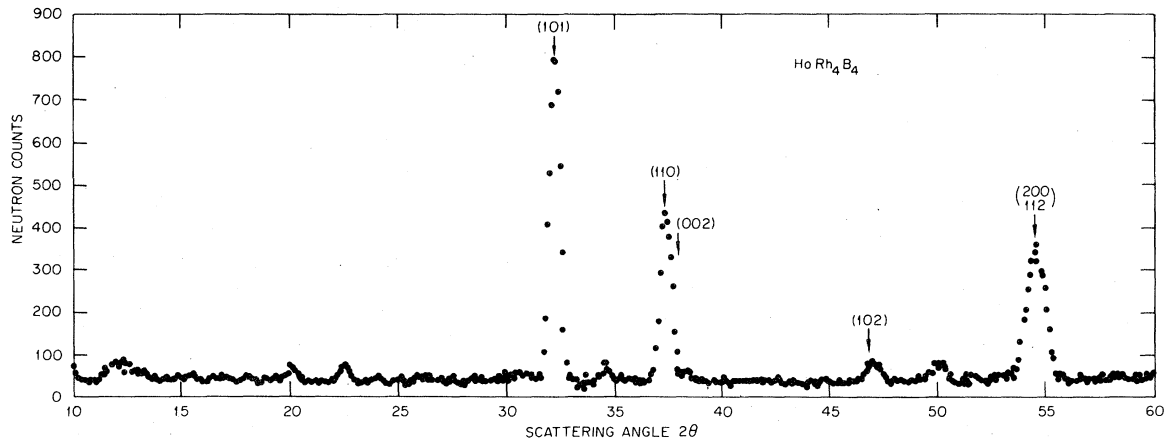


FIG. 2. Powder diffraction pattern for HoRh₄B₄ measured at 1.7 K.

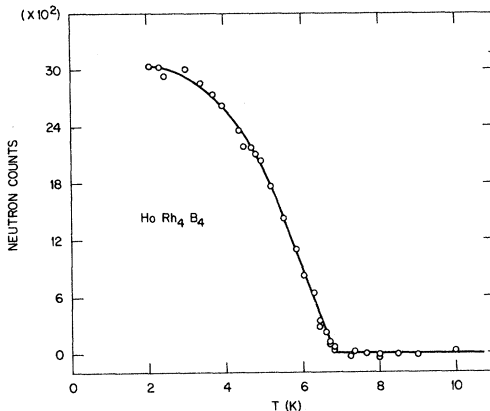


FIG. 3. Magnetic intensity of the (101) reflection for HoRh_4B_4 as a function of temperature.

model and other evidence for the mean-field nature of the magnetic transition is the subject of a paper by Ott *et al.*²⁸ and thus we will not discuss this aspect of the magnetic ordering any further here.

ErRh_4B_4

ErRh_4B_4 becomes a superconductor at about 8.7 K and orders magnetically below about 1 K.¹ Neutron scattering measurements by Moncton *et al.*²² showed that this material developed long-range ferromagnetism in which the Er^{+3} moments ordered in the basal plane with a saturation moment of $5.6\mu_B$ per Er atom at low temperatures. Further measurements^{29,30} on this material revealed that peaks in the neutron scattering pattern developed at small scattering angles for temperatures near the transition, thus confirming theoretical predictions by Blount and Varma³ that an oscillatory magnetic state may develop in the neighborhood of the transition. We have not made powder diffraction measurements on this material except for magnetic field dependent measurements at 1.79 K which is above the magnetic ordering temperature.³¹ From these measurements it was found that

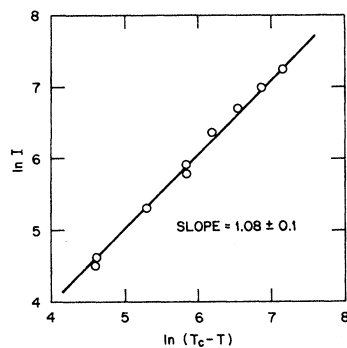


FIG. 4. Intensity vs temperature relation for HoRh_4B_4 .

long-range magnetic order occurs for fields larger than 0.75 kOe, again with the moment direction oriented in the basal plane. Large thermal hysteresis was found in the magnetic order parameter.

Recently, a single crystal of ErRh_4B_4 has been grown and neutron scattering measurements have been made which give a clearer picture of the nature of the magnetic transition in this material.³² We shall only summarize some of the main features of the magnetic scattering found for this single-crystal material since full details will be published elsewhere. For temperatures below 1.2 K but above 0.7 K, ErRh_4B_4 shows both long-range ferromagnetic order and superconductivity. A transverse, linearly polarized, sinusoidally modulated structure with a wavelength of 100 \AA and making a 45° angle with the c axis and each of the equivalent a axes is also found in this temperature region. This structure disappears rapidly below 0.7 K leaving only long-range ferromagnetism. Superconductivity is also destroyed at this transition. The order parameter curve determined from the (101) reflection shows considerable hysteresis in the temperature region between 0.9 and 0.7 K. Other features of the magnetic transition have been measured using the single crystal but the above information is sufficient for comparison with our measurements on the $\text{Ho}_{1-x}\text{Er}_x\text{Rh}_4\text{B}_4$ alloys since only powder measurements have been made in this alloy system. The heat-capacity measurements on ErRh_4B_4 (Refs. 16 and 33) show a sharp spike-shaped anomaly at 0.93 K superimposed on a rather broad structure. This broad structure is obviously an indication that the magnetic transition for ErRh_4B_4 is not a simple nature.

$\text{Ho}_{0.6}\text{Er}_{0.4}\text{Rh}_4\text{B}_4$

This compound is a reentrant superconductor with the reentrant superconducting transition taking place at 3.60 K. The heat-capacity measurements show the same type of sawtooth-shaped feature that was observed for HoRh_4B_4 but, in addition, there is a large narrow spike at the reentrant transition temperature.¹⁶ A preliminary account of our neutron scattering measurements for this compound is given in Ref. 34.

A number of different diffraction patterns were obtained for this compound with various resolutions. Most of the data were taken with the usual setup using pyrolytic graphite as monochromator and filter, but some data were obtained with a Be monochromator which gave better resolution. Figure 5 shows a high-resolution powder diffraction scan of the (101), (110), and (002) peaks at 4.2 and 1.6 K. These peaks all have small nuclear components as observed in the 4.2 K data. Large magnetic (101) and (110) peaks are found at 1.6 K showing long-range ferromagnetic order; however, no (002) peak is found.

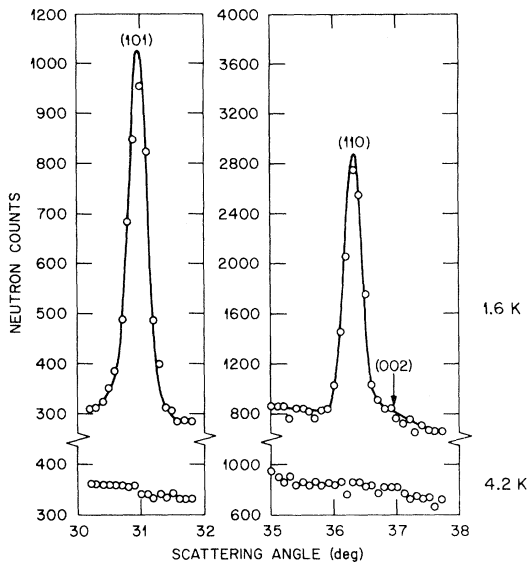


FIG. 5. Powder diffraction scans for $\text{Ho}_{0.6}\text{Er}_{0.4}\text{Rh}_4\text{B}_4$ for 1.6 and 4.2 K.

This shows that the moment is parallel to the c axis. Figure 6 shows a high-resolution scan of some higher angle peaks taken at 4.2 and 1.6 K. No additional peak broadening is found upon magnetic ordering showing that long-range ferromagnetic order has been established. We can put a lower limit on the

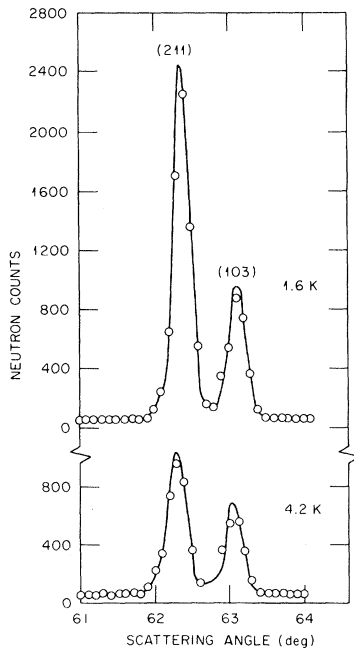


FIG. 6. Higher angle high-resolution diffraction scans for $\text{Ho}_{0.6}\text{Er}_{0.4}\text{Rh}_4\text{B}_4$ showing that the magnetic order is long range.

range of the magnetic order by using $\Delta Q = (4\pi/\lambda)\cos\theta\Delta\theta$, where λ is the incident neutron wavelength and θ is the scattering angle. The peak halfwidth is 0.3 deg giving a momentum uncertainty ΔQ of 0.01 \AA^{-1} . This width is the instrumental resolution which is consistent with the width of the nuclear peaks in the diffraction pattern. We should be able to easily see broadening equal to one-half our resolution giving us a correlation range of $2/0.01 \text{ \AA}^{-1} = 200 \text{ \AA}$.

An analysis of the diffraction pattern has been performed to give us the ordered moment. The diffraction pattern was obtained by placing the sample in a thin flat sample cell. For this geometry the scattered intensities for the nuclear peaks are given by

$$I_{hkl} = C \frac{j}{\sin^2\theta} |F_n|^2 e^{-at \sec\theta},$$

where j is the multiplicity factor for each reflection, t is the sample thickness, a is the linear absorption coefficient, and C is a constant. The coefficient a was determined by transmission measurements through the sample cell, while the constant C was established for each reflection from the measured intensity of the 4.2-K powder pattern. The magnetic structure factors F_m could then be established from the 1.6-K diffraction pattern and a magnetic moment determined for each reflection using Eq. (1). Good internal consistency is obtained for the various reflections and the data are consistent with a moment of $(5.0 \pm 0.5) \mu_B$ at 1.6 K. This moment is considerably below the free-ion moment for Ho or Er but similar to that found for ErRh_4B_4 . One possibility is that only the Ho ions are magnetically ordered at 1.6 K, in which case the magnetic moment per Ho ion would be $8.3 \mu_B$ which is in reasonable agreement with the value found for Ho in HoRh_4B_4 .²⁵ We will see that in $\text{Ho}_{0.3}\text{Er}_{0.7}\text{Rh}_4\text{B}_4$ magnetic ordering first occurs along the c axis and then within the basal plane at a lower temperature. This suggests that the Ho, with its preference for ordering along the c axis, orders first at a higher temperature and then Er, with its preference for ordering within the basal plane, orders at a lower temperature. Thus, while the neutrons cannot distinguish between Er or Ho, it is reasonable to assume a model for the $\text{Ho}_{1-x}\text{Er}_x\text{Rh}_4\text{B}_4$ alloy system in which Ho is responsible for magnetic ordering along the c axis and Er responsible for ordering perpendicular to the c axis.

Figure 7 shows the intensity of the (101) powder peak as a function of temperature. This gives us a measure of the order parameter for the magnetic system. Upon cooling no long-range magnetic order is found above 3.60 K. At 3.60 K the magnetic intensity jumps suddenly to a finite value and then increases nearly linearly as the temperature is lowered to about 2.5 K. Below 2.5 K the intensity rounds off and appears to saturate at about 1.6 K which was the lowest

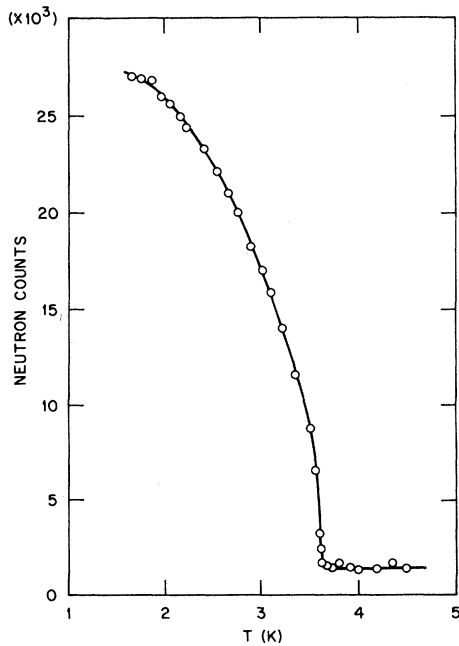


FIG. 7. Magnetic intensity of the (101) reflection for $\text{Ho}_{0.6}\text{Er}_{0.4}\text{Rh}_4\text{B}_4$ as a function of temperature.

temperature attained in the experiment. As mentioned above, the magnetic order parameter might increase again at some lower temperature but the heat-capacity measurements¹⁶ show no anomalies between 0.5 K, the low temperature limit of the heat-capacity experiments, and 1.6 K.

Figure 8 shows a more detailed plot of the magnetic intensity in the neighborhood of the transition. The error bars are about the size of the points and the temperature stability better than 0.005 K. We see clearly the jump in the magnetic intensity at 3.60 K and the change in slope of the intensity-versus-temperature curve in the neighborhood of the transition. Since the magnetic scattering intensity is proportional to the square of the magnetic moment the fast rise in intensity signifies a rapid increase in the ordered moment. In fact the system develops almost half its saturated moment in a temperature interval of about 0.05 K. Little hysteresis is found in the transition temperature, but hysteresis is found in the magnetization developed at a given temperature. This hysteresis disappears around 2 K as saturation is approached. The linear slope in the temperature range between 2.5 and 3.4 K is reminiscent of that found near the transition in HoRh_4B_4 . This suggests that the transition in $\text{Ho}_{0.6}\text{Er}_{0.4}\text{Rh}_4\text{B}_4$ is mean-field-like in the range below 3.4 K, but above this temperature the mean-field transition is preempted by a first-order transition. If the linear slopes are extended to zero counts one obtains a transition tempera-

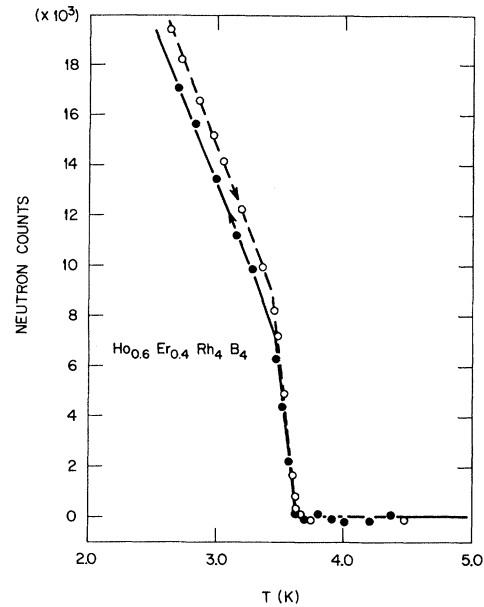
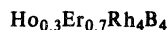


FIG. 8. Expanded view of the temperature dependence of the (101) reflection for $\text{Ho}_{0.6}\text{Er}_{0.4}\text{Rh}_4\text{B}_4$ in the neighborhood of the transition.

ture of about 4.0 K which would be the transition temperature if the first-order transition did not take place. If one uses 4.0 K for the transition temperature the exponent α in Eq. (4) again is very nearly unity confirming the mean-field-like behavior of the magnetic order parameter over the temperature range where the slope is linear. We notice the dashed line in Fig. 1 obtained by extrapolation from the Ho-rich alloys suggests a transition temperature of around 4.0 K. Our data then suggest that $\text{Ho}_{0.6}\text{Er}_{0.4}\text{Rh}_4\text{B}_4$ would order magnetically at 4.0 K with a mean-field transition but that superconductivity reduces the ordering temperature to 3.60 K. This shows directly how magnetic ordering is suppressed by superconductivity.

The heat-capacity spike coincides with the development of long-range magnetic order and the disappearance of superconductivity at 3.60 K. There is no coexistence of superconductivity and long-range magnetic order in $\text{Ho}_{0.6}\text{Er}_{0.4}\text{Rh}_4\text{B}_4$. This material provides an example of long-range ferromagnetic order destroying superconductivity with a sharp first-order transition. Small-angle scattering measurements were made near the transition to look for low-angle satellites such as those found in ErRh_4B_4 .²⁹ No evidence of satellites was found although a better experiment on a spectrometer designed for small-angle scattering should be carried out. In any case, this material orders quite differently from ErRh_4B_4 which has a smooth order-parameter curve with no sudden jumps in magnetization.



The heat capacity of this material shows two peaks.¹⁶ A sharp spike superimposed on a broad feature is found at about 1.2 K; this temperature coincides with the destruction of superconductivity. An additional rounded maximum is found at a lower temperature, with the maximum at 0.74 K. These two broad heat-capacity features suggest two separate magnetic transitions and serve to remind us that the Ho and Er ions may order independently and in different directions in the alloy. In fact, we now know that the Ho-rich compounds order along the *c* axis, while ordering in the basal plane is found in ErRh_4B_4 . We thus have a magnetic material that has two components whose respective magnetic anisotropies are orthogonal. This is then similar to the $\text{Fe}_{1-x}\text{Co}_x\text{Cl}_2$ system studied by Wong *et al.*,³⁵ except in our case we have superconductivity in addition. Thus not only do we have to consider the problem of the interaction of magnetism and superconductivity but the interaction of the field produced by one set of ions on the other set. The mixed anisotropy problem has been treated by Fishman and Aharony³⁶; however, the results of Wong *et al.*³⁵ do not seem to support the conclusion of a "decoupled tetracritical point."

Powder diffraction peaks for the (101), (110), and (002) reflection for $\text{Ho}_{0.3}\text{Er}_{0.7}\text{Rh}_4\text{B}_4$ are shown in Fig. 9. We see again strong magnetic peaks at 0.4 K and notice that a strong (002) peak is visible showing that at 0.4 K there is some ordering that is not along the *c* axis. The diffraction peaks are again resolution limited showing that the magnetic order is long range in nature.

The magnetic intensity of the (101) reflection is shown in Fig. 10 which gives us the order parameter

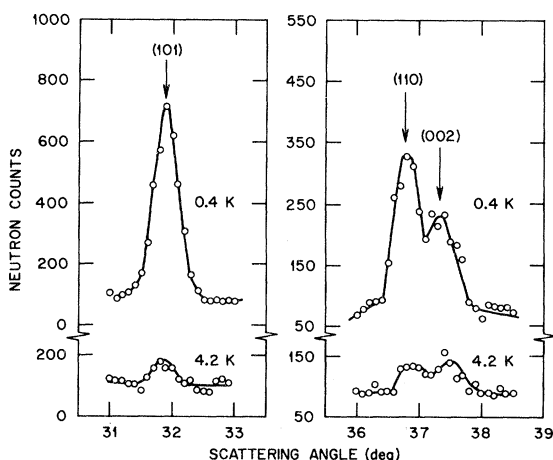


FIG. 9. Powder diffraction scans for $\text{Ho}_{0.3}\text{Er}_{0.7}\text{Rh}_4\text{B}_4$ for 0.4 K and 4.2 K.

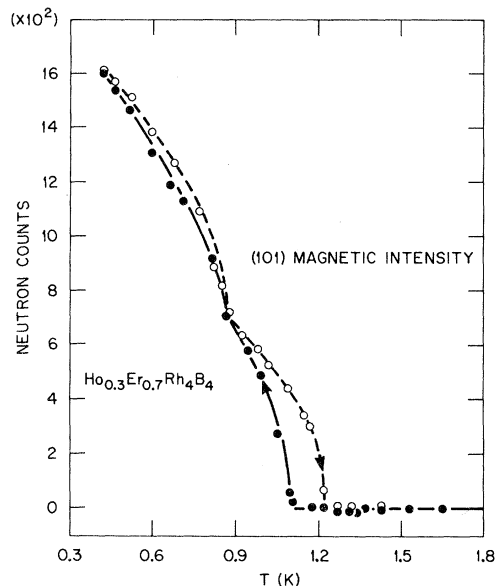


FIG. 10. Magnetic intensity of the (101) reflection for $\text{Ho}_{0.3}\text{Er}_{0.7}\text{Rh}_4\text{B}_4$ as a function of temperature.

of the magnetic system. The (101) reflection is sensitive to order both along the *c* axis and in the basal plane so that ordering in either direction will make a contribution to the reflection. We notice that as the temperature is decreased, magnetic order becomes evident at about 1.1 K which is the temperature the ac magnetic susceptibility measurements show that superconductivity is destroyed.¹² We note that no evidence of critical fluctuations is apparent and that the magnetic intensity curve rises sharply in a manner similar to that for $\text{Ho}_{0.4}\text{Er}_{0.6}\text{Rh}_4\text{B}_4$. At about 0.85 K there is a change in slope in the order-parameter curve suggesting another transition. The data taken upon warming show small hysteresis that seems to disappear at 0.85 K. Above 0.85 K large hysteresis is found and the temperature at which ferromagnetism is lost is consistent with the temperature the ac magnetic susceptibility measurements give for the onset of superconductivity.¹⁵ The largest hysteresis in the ac magnetic susceptibility is found near this alloy composition. The large spike in the heat capacity¹⁶ occurs at the temperature at which ferromagnetism is lost and superconductivity regained as the sample is warmed. The change in slope of the order-parameter curve in the neighborhood of 0.85 K occurs at about the same temperature that the rounded feature is found in the heat-capacity measurements.¹⁶

By looking at the temperature dependence of reflections other than the (101) we can examine the ordering along the *c* axis separately from that along the basal plane. Figure 11 shows the temperature depen-

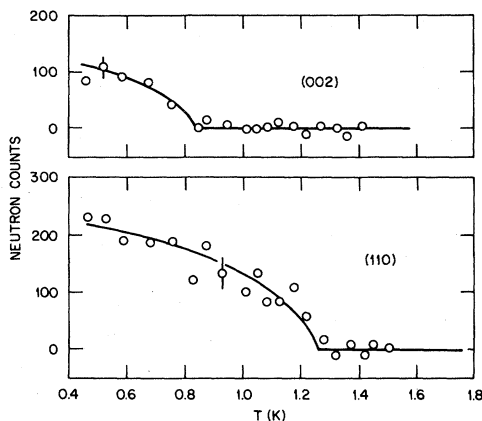


FIG. 11. Temperature dependence of the magnetic components of the (002) and (110) reflections plotted as a function of temperature.

dence of the magnetic components of the (110) and (002) reflections. As the sample is warmed from about 0.4 K, we see that the (002) reflection disappears at about 0.85 K while the (110) reflection persists until the temperature is increased to above 1.2 K. This tells us that ordering takes place only along the c axis above 0.85 K but that ordering exists with a component perpendicular to the c axis below 0.85 K. It appears then that the Ho orders first in $\text{Ho}_{0.3}\text{Er}_{0.7}\text{Rh}_4\text{B}_4$, since Ho favors ordering along the c axis, and that the Er orders in the basal plane at about 0.85 K. MacKay *et al.*¹⁶ suggested that this type of ordering was consistent with the phase boundaries for the alloy system. The neutron results now give us more support for this interpretation of the magnetic ordering. The two different types of ordering complicate the analysis of the low-temperature diffraction pattern. However, by examining the strength of the (002) reflection we find that the c -axis moment is $(2.3 \pm 0.5) \mu_B$ at the lowest temperature measured. If the Ho is responsible for this moment it would mean that the Ho orders with about the same moment as in HoRh_4B_4 . The moment not along c which we will assume is in the basal plane is $(3.6 \pm 0.5) \mu_B$. If the Er was responsible for this mo-

ment, it would imply that the Er carries about the same moment as the Er in ErRh_4B_4 at low temperatures. Since the Ho appears to order first, it means that we are still on the Ho-rich side of the multicritical point in the magnetic phase diagram. It would be interesting to examine other alloy compositions nearer the multicritical point.

CONCLUSION

Using neutron scattering techniques we have examined the magnetic transition for compounds in the $(\text{Ho}_{1-x}\text{Er}_x)\text{Rh}_4\text{B}_4$ pseudoternary system. We find a wide variety of behavior ranging from mean-field behavior for HoRh_4B_4 to complicated behavior with more than one type of ordering for $\text{Ho}_{0.3}\text{Er}_{0.7}\text{Rh}_4\text{B}_4$. Our results are consistent with the picture that Ho orders along the c axis with nearly its full free-ion moment in the alloy system while Er orders in the basal plane but with a moment reduced from the free-ion value. Ordering along the c axis results in the destruction of superconductivity in a sharp transition at the same temperature that a sharp spike appears in heat capacity.¹⁶ Hysteresis found for the ordering temperature in $\text{Ho}_{0.3}\text{Er}_{0.7}\text{Rh}_4\text{B}_4$ is consistent with that found in the ac magnetic susceptibility measurements.¹⁵ The competing anisotropies of Ho and Er in the alloys are probably responsible for the minimum in the magnetic ordering temperature between the Er and Ho end points of the phase diagram. Alloy compositions near this minimum are near a multicritical point in the phase diagram and both orthogonal magnetic anisotropies and superconductivity play an important role in the nature of the magnetic transition.

ACKNOWLEDGMENTS

This research was sponsored in part by the Division of Materials Sciences, U.S. Department of Energy, under Contract No. W-7405-eng-26 with the Union Carbide Corporation, U.S. Department of Energy under Contract No. DE-AT03-76ER70227, and the National Science Foundation under Grant No. NSF/DMR77-08469.

*Present address: Corporate Research Laboratories, Exxon Research and Engineering Company, P. O. Box 45, Linden, N.J. 07037.

¹W. A. Fertig, D. C. Johnston, L. E. DeLong, R. W. McCallum, M. B. Maple, and B. T. Matthias, Phys. Rev. Lett. **38**, 987 (1977).

²M. Ishikawa and O. Fischer, Solid State Commun. **23**, 37 (1977).

³E. I. Blount and C. M. Varma, Phys. Rev. Lett. **42**, 1079 (1979); Phys. Rev. Lett. **43**, 1843(E) (1979).

⁴M. Tachiki, H. Matsumoto, and H. Umezawa, Phys. Rev. **20**, 1915 (1979).

⁵M. V. Jaric and M. Belic, Phys. Rev. Lett. **42**, 1015 (1979).

⁶M. Tachiki, A. Kotani, H. Matsumoto, and H. Umezawa, Solid State Commun. **31**, 927 (1979).

⁷M. Tachiki, A. Kotani, H. Matsumoto, and H. Umezawa,

- Solid State Commun. 32, 599 (1979).
- ⁸H. Matsumoto, H. Umezawa, and M. Tachiki, Solid State Commun. 31, 157 (1979).
- ⁹C. G. Kuper, M. Revzen, and A. Ron, Phys. Rev. Lett. 44, 1545 (1980).
- ¹⁰S. Maekawa, M. Tachiki, and S. Takahashi, J. Magn. Mater. 13, 324 (1979).
- ¹¹H. S. Greenside, E. I. Blount, and C. M. Varma, Phys. Rev. Lett. 46, 49 (1981).
- ¹²S. Maekawa and C. Y. Huang, in *Crystalline Electric Field and Structural Effects in *f*-Electron systems*, edited by J. E. Crow, R. P. Guertin, and T. W. Mihalisin (Plenum, New York, 1980), p. 561.
- ¹³S. Maekawa, J. L. Smith, and C. Y. Huang, Phys. Rev. B. 22, 164 (1980).
- ¹⁴B. Schuh and N. Grewe, Solid State Commun. 37, 145 (1981).
- ¹⁵D. C. Johnston, W. A. Fertig, M. B. Maple, and B. T. Matthias, Solid State Commun. 26, 141 (1978).
- ¹⁶H. B. MacKay, L. D. Woolf, M. B. Maple, and D. C. Johnson, Phys. Rev. Lett. 42, 918 (1979).
- ¹⁷R. N. Shelton, C. O. Segre, and D. C. Johnston, Solid State Commun. 33, 843 (1980).
- ¹⁸H. Adrian, K. Miller, and G. Salmann-Ischenko, in *Proceedings of the First International Conference on Ternary Superconductors, Lake Geneva, September 24–26*, edited by G. K. Shenoy, B. D. Dunlap, and F. Y. Fradin (Elsevier/North-Holland, New York, 1981).
- ¹⁹W. Adrian, K. Miller, and G. Salmann-Ischenko, Phys. Rev. B 22, 4424 (1980).
- ²⁰M. Ishikawa, Phys. Lett. A 74, 263 (1979).
- ²¹J. M. Vandenberg and B. T. Matthias, Proc. Nat. Acad. Sci. U.S.A. 74, 1336 (1977).
- ²²D. E. Moncton, D. B. McWhan, J. Eckert, G. Shirane, and W. Thomlinson, Phys. Rev. Lett. 39, 1164 (1977).
- ²³W. Marshall and S. W. Lovesey, *Theory of Thermal Neutron Scattering* (Oxford, London, 1971).
- ²⁴C. Stassis, H. W. Deckman, B. N. Harmon, J. P. Desclaux, and A. J. Freeman, Phys. Rev. B 15, 369 (1977).
- ²⁵G. H. Lander, S. K. Sinha, and F. Y. Fradin, J. Appl. Phys. 50, 1990 (1979).
- ²⁶M. B. Maple, H. C. Hamaker, D. C. Johnston, H. B. MacKay, and L. D. Woolf, J. Less Common Met. 62, 251 (1978).
- ²⁷H. R. Ott, L. D. Woolf, M. B. Maple, and D. C. Johnston, J. Low Temp. Phys. 39, 383 (1980).
- ²⁸H. R. Ott, G. Keller, W. Odoni, L. D. Woolf, M. B. Maple, D. C. Johnston, and H. A. Mook (unpublished).
- ²⁹D. E. Moncton, D. B. McWhan, P. H. Schmidt, G. Shirane, W. Thomlinson, M. B. Maple, H. B. MacKay, L. D. Woolf, Z. Fisk, and D. C. Johnston, Phys. Rev. Lett. 45, 2060 (1980).
- ³⁰D. E. Moncton, G. Shirane, and W. Thomlinson, J. Magn. Mater. 14, 179 (1979).
- ³¹H. A. Mook, M. B. Maple, Z. Fisk, and D. C. Johnston, Solid State Commun. 36, 287 (1980).
- ³²S. K. Sinha, G. W. Crabtree, D. G. Hinks, and H. A. Mook (unpublished).
- ³³L. D. Woolf, D. C. Johnston, H. B. MacKay, R. W. McCallum, and M. B. Maple, J. Low Temp. Phys. 35, 651 (1979).
- ³⁴H. A. Mook, W. C. Koehler, M. B. Maple, Z. Fisk, and D. C. Johnston, in *Superconductivity in *d*- and *f*-Band Metals*, edited by H. Suhl and M. B. Maple (Academic, New York, 1980), p. 427.
- ³⁵Po-zen Wong, P. M. Horn, R. J. Birgeneau, C. R. Safinya, and G. Shirane, Phys. Rev. Lett. 45, 1974 (1980).
- ³⁶S. Fishman and A. Aharony, Phys. Rev. 18, 3507 (1978).